**Supporting Information**

# Targeted delivery of insoluble cargo (paclitaxel) by PEGylated chitosan-nanoparticles grafted with Arg-Gly-Asp (RGD)

Pi-Ping Lv,[†,‡,§] Yu-Feng Ma,[‖,§] Rong Yu,[‖] HuaYue,[†] De-Zhi Ni,[†,‡] Wei Wei,[†,*] and Guang-Hui Ma[†,*]

[†]National Key Laboratory of Biochemical Engineering, Institute of Process Engineering, Chinese Academy of Sciences, Beijing, 100190, PR China

[‖] Key Laboratory of Drug Targeting and Drug Delivery System, Ministry of Education,West China School of Pharmacy, Sichuan University, Chengdu, 610041, China

[‡]Graduate University of Chinese Academy of Sciences, Beijing, 100049, PR China

[§]Both authors contributed equally

[*]Corresponding authors. Tel. /fax: +86 10 82627072.

E-mails: weiwei@home.ipe.ac.cn; ghma@home.ipe.ac.cn.

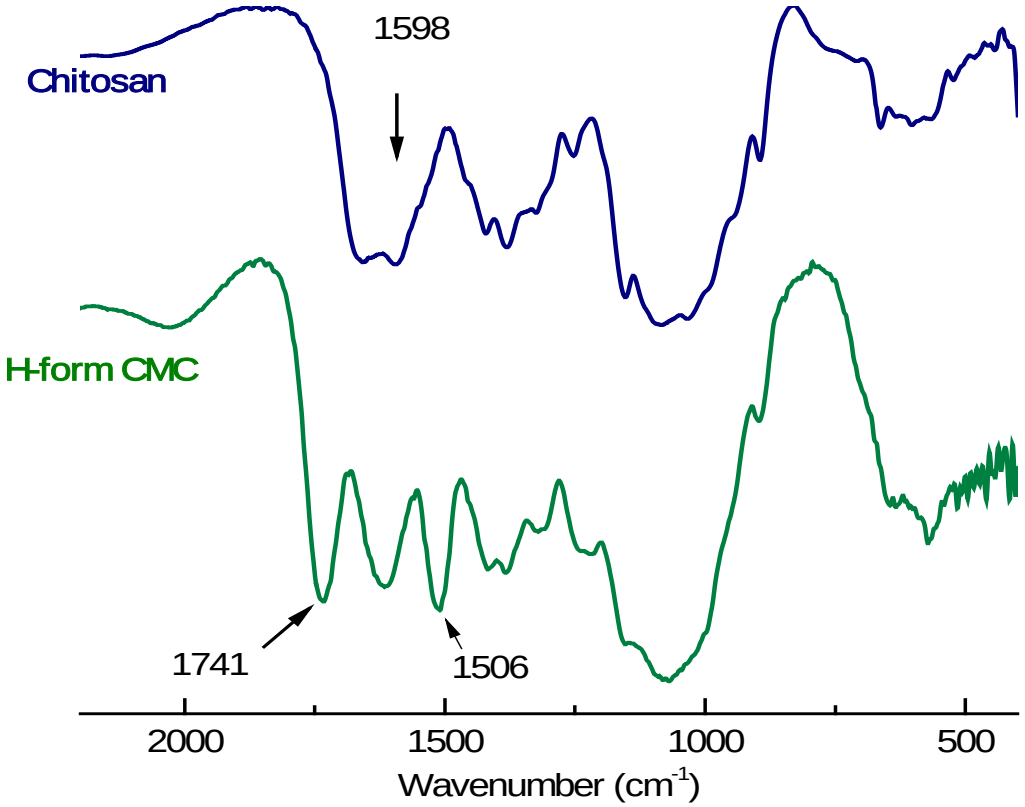


Fig. S1. FT/IR spectrum of chitosan and H-form CMC.

Chitosan exhibits characteristic adsorption of amino group at 1598 $cm^{-1}$. In the spectrum of H-form CMC, a new band appears around 1741 $cm^{-1}$, which can be assigned to the carboxylmethyl group (–COOH). The band at 1506 $cm^{-1}$ is the characteristic of $–NH_3^+$, confirming that the carboxylmethyl group was successfully coupled on the –OH position.[1]

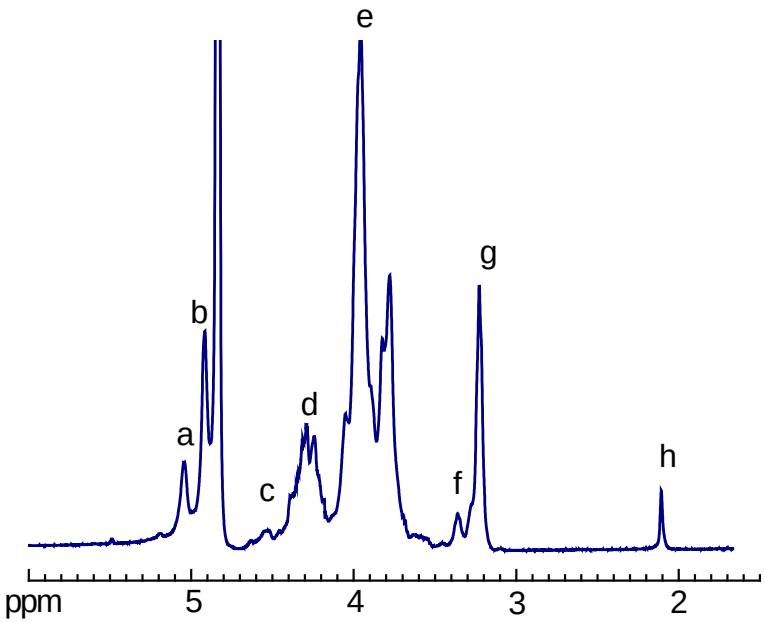


Fig. S2. $^{1}$H NMR analysis of CMC in $D_2O/CD_3COOD$. Signals in the 500 MHz $^{1}$H-NMR spectrum of CMC can be assigned as follow: δ=5.05 (a, H1D), δ=4.90 (b, H1A), δ=4.15~4.65 (c and d, H3' and H6'), δ=3.70~4.01 (e, H3, H4, H5, H6), δ=3.35 (f, H2'), δ=3.20 (g, H2D), δ=2.10 (h, H2'). H' refers to protons of a carboxymethylated unit. The A and D refer to the acetylated and deacetylated units, respectively.

The substitution of carboxymethyl groups can be determined from the $^{1}$H NMR spectra using the method previously reported.[1] The calculated equations are as follows:

(1) $f_6 = (1/2)\ (I_d - I_c)/(I_b + I_g)$

(2) $f_3 = I_c/(\ I_b + I_g)$

(3) $f_2 = (1/2)I_f/(I_b + I_g)$

(4) $F = f_6 + f_3 + f_2$

The $f_6$, $f_3$ and $f_2$ are the fractions of carboxymethylation at the position of 6-O-, 3-O- and 2-N-, respectively. F is the total fraction of carboxymethylation. The substitution degree on 6-O-, 3-O- and 2-N- are 53.90%, 4.65% and 4.95%, respectively.The total substitution degree of carboxymethyl groups (F) was 63.5%, providing enough carboxyl for the subsequent modification.

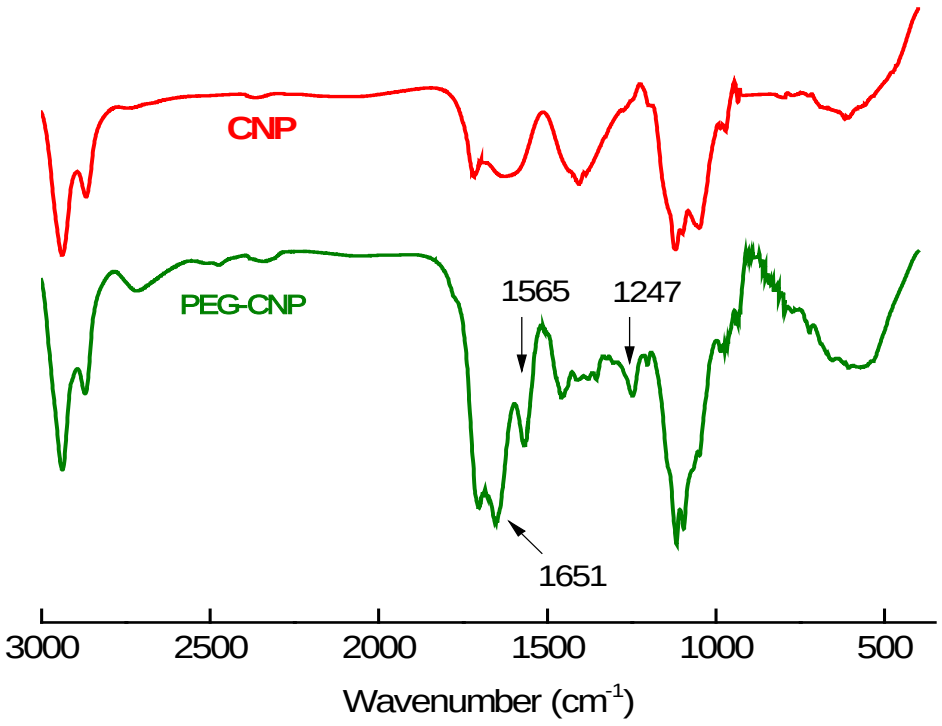


Fig. S3. FT/IR spectrum of CNP and PEG-CNP.

Fig. S3 shows the FT/IR spectrum of CNP and PEG-CNP to confirm the conjunction of PEG chain onto the nanoparticles surface. Compared with CNP, three new peaks of amide bond were observed in PEG-CNP: the C=O stretching vibration for the amide bond is at 1651 $cm^{-1}$, combination of N-H deformation and C-N stretching vibrations are observed at 1565 $cm^{-1}$, and the peak at 1247 $cm^{-1}$ is attributed to the mixed vibrations of C-N stretching and N-H bending.[2] These results demonstrated that PEG chains were successfully grafted onto the surface of CNP via the amide linkage.

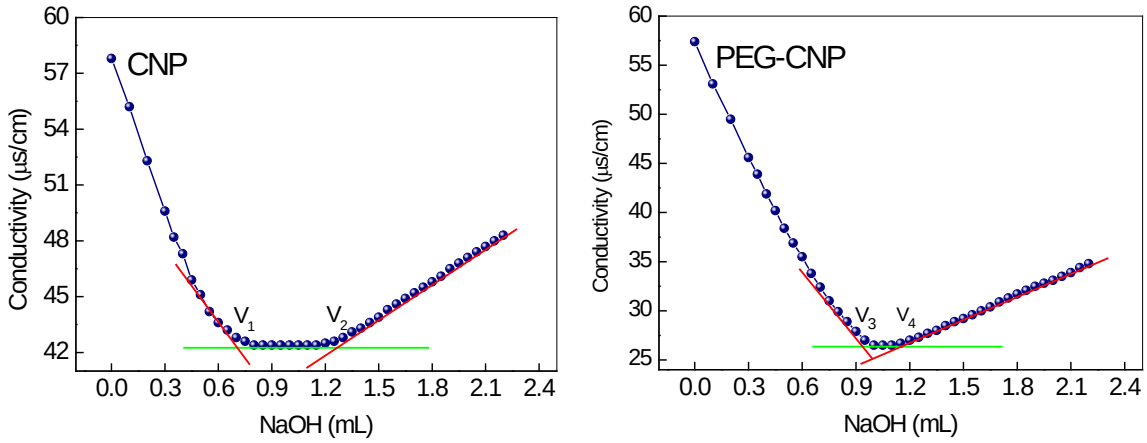


Fig. S4. The Conductometric titration of the CNP and PEG-CNP.

Method:We performed conductometric titration to determine the carboxyl groups of CNP and PEG-CNP by Multi-parameter measuring instrument (ProLab 4000, SCHOTT). 20 mg of freeze-dried sample (CNP or PEG-CNP) wassuspended in 15 mL of NaCl solution(1 mM).NaOH (Freshlyprepared from Acculute standard volumetric concentrates, 2 mM) was used as titrant. The pH of suspension was adjusted to 4.0, and nitrogen was bubbled through the solution for 1/2 h prior to titrationto remove dissolved carbon dioxide from the system. Nitrogen was blown gently on the sample during the titration to maintain an inert atmosphere.During titration, the suspension was tenderly stirred with a magnetic stirrer at 25 °C. The titration was performed by adding 2 mM NaOH in steps of 0.05 mL (0.1 mL of NaOH in the first three steps) with 1.0 min intervals. The conductivity value was recorded after each addition. The total carboxyl group content (X) of CNP or PEG-CNP (20 mg) was calculated by: $X=C_{OH}\times V_t$, where the $C_{OH}$ is the concentration of sodium hydroxide solution, $V_{t,CNP}=V_2-V_1$ (or $V_{t,PEG\text{-}CNP}=V_3-V_4$).

Result: About 64% carboxyl was substituted by the PEG chain.

Table S1. Elemental analysis of different nanoparticles

| NPs | Experimental value (mean, n=3) | | Saturated value | |
|---|---|---|---|---|
| | C (%) | S (%) | C(%) | S(%) |
| CNP | 48.846 | 0 | 49.057 | 0 |
| PEG-CNP | 45.330 | 0 | 45.205 | 0 |
| RGD-PEG-CNP | 45.525 | 0.104 | 45.304 | 0.173 |

According to the data, we calculated the grafting density of cyclic RGD peptide, and approximately 0.5-0.6 cyclic RGD peptide molecule per PEG chain was grafted.

Table S2. Physicochemical characteristics of different PTX-loaded nanoparticles

| NPs | LE (%) | Size (nm) | PDI | ζ potential (mV) |
|---|---|---|---|---|
| CNP | 35.6±4.3 | 125.4±2.6 | 0.037±0.004 | -32.73±1.35 |
| PEG-CNP | 33.5±2.7 | 140.2±3.5 | 0.053±0.006 | +2.19±4.15 |
| RGD-PEG-CNP | 30.2±2.9 | 142.5±4.1 | 0.056±0.005 | +1.97±3.18 |

The obtained three PTX-loaded nanoparticles were characterized in terms of size, ζ potential and LE, and the detailed results are shown in Table S2. All three PTX-loaded nanoparticles exhibited a very narrow size distribution (PDI<0.1), ensuring the batch-to-batch consistencies. The size of PEG-CNP:PTX or RGD-PEG-CNP:PTX was enhanced slightly (140.2 and 142.5 nm, respectively) over CNP:PTX (125.4 nm) due to the couple of PEG chain and the graft of cyclic RGD peptide. ζ potential of PEG-CNP:PTX was close to neutrality, indicating the presence of PEG chains can shield the negative charges presented at the CNP surface.

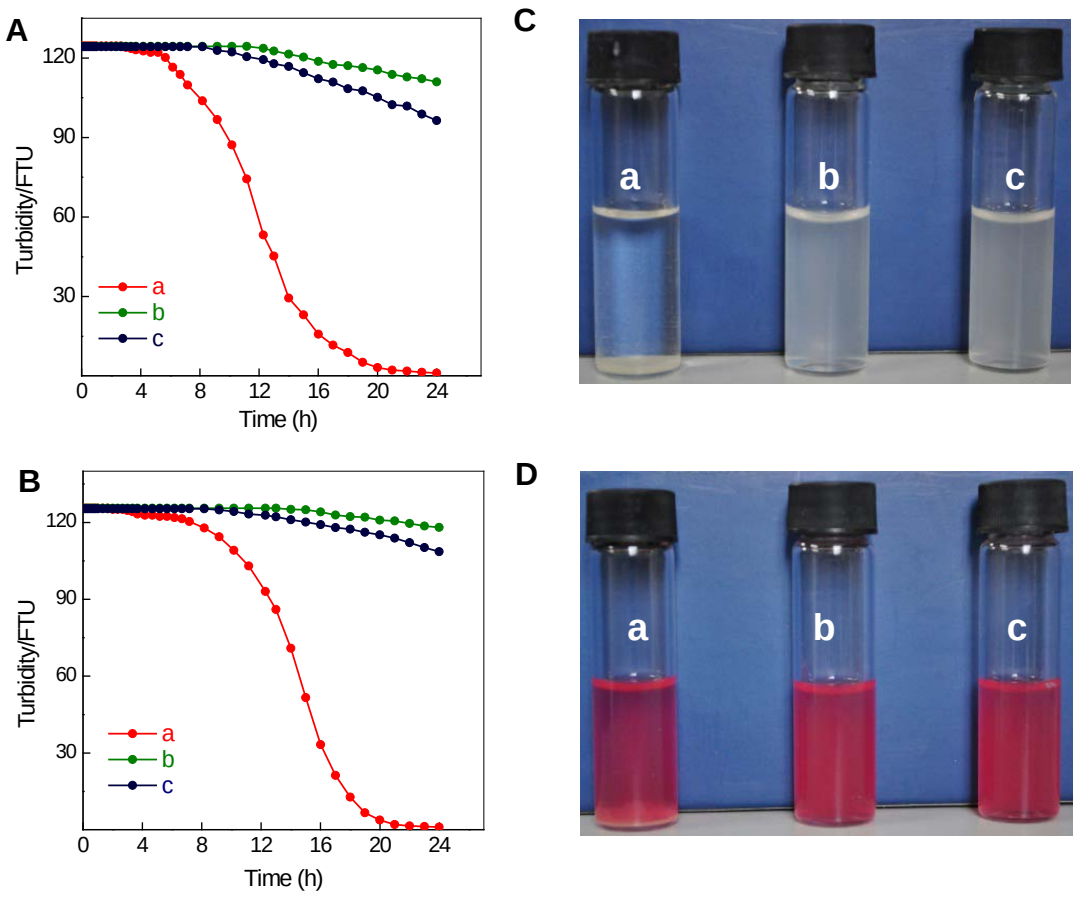


Fig. S5. The kinetic turbidity of CNP (a), PEG-CNP (b) and RGD-PEG-CNP (c) in PBS (pH7.2, A) and cell culture medium (DMEM) containing 10% FBS (B) at 37 $^{o}$C. C and D were the corresponding suspensions kept at 37 $^{o}$C for 24 h.

Rapid decreases of turbidity (in PBS and DMEM) were observed in the group of CNP, while this phenomenon did not arise in PEGylated nanoparticles (PEG-CNP and RGD-PEG-CNP). Additionally, these two nanoparticles are still well dispersed in all mediums after 24 h, whereas lots of aggregates are present in the suspension of CNP. We concluded that the coupling of PEG chains on the nanoparticles could provide hydrophilic interface, and therefore, stabilize the nanosuspension.

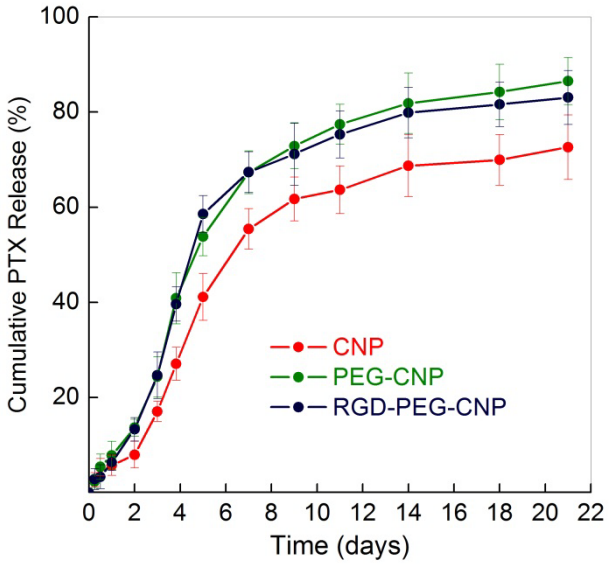


Fig. S6 The release profiles of PTX from different PTX-loaded nanoparticles.

The release profiles of different PTX-loaded nanoparticles (CNP:PTX, PEG-CNP:PTX and RGD-PEG-CNP:PTX) were performed in vitro. As shown in the Fig. S6, no significant burst release of PTX was observed among these three PTX-loaded nanoparticles, which might be attributed to the in-situ crystallization of PTX.Once PEGylated, the release rate of PTX from nanoparticles increased due to the improvement of hydrophilicity via PEG chain(Moneghini,M.; Kikic, I.; Voinovich, D.; Perissutti, B.; et al.*International Journal of Pharmaceutics* 2001, *222*, 129-138). In addition, the RGD conjunction did not influence the drug release.After incubation for 9 days, the cumulative amount of PTX released from both PEGylated nanoparticleswere above70%, which would contribute to the enhancement of antitumor effects.

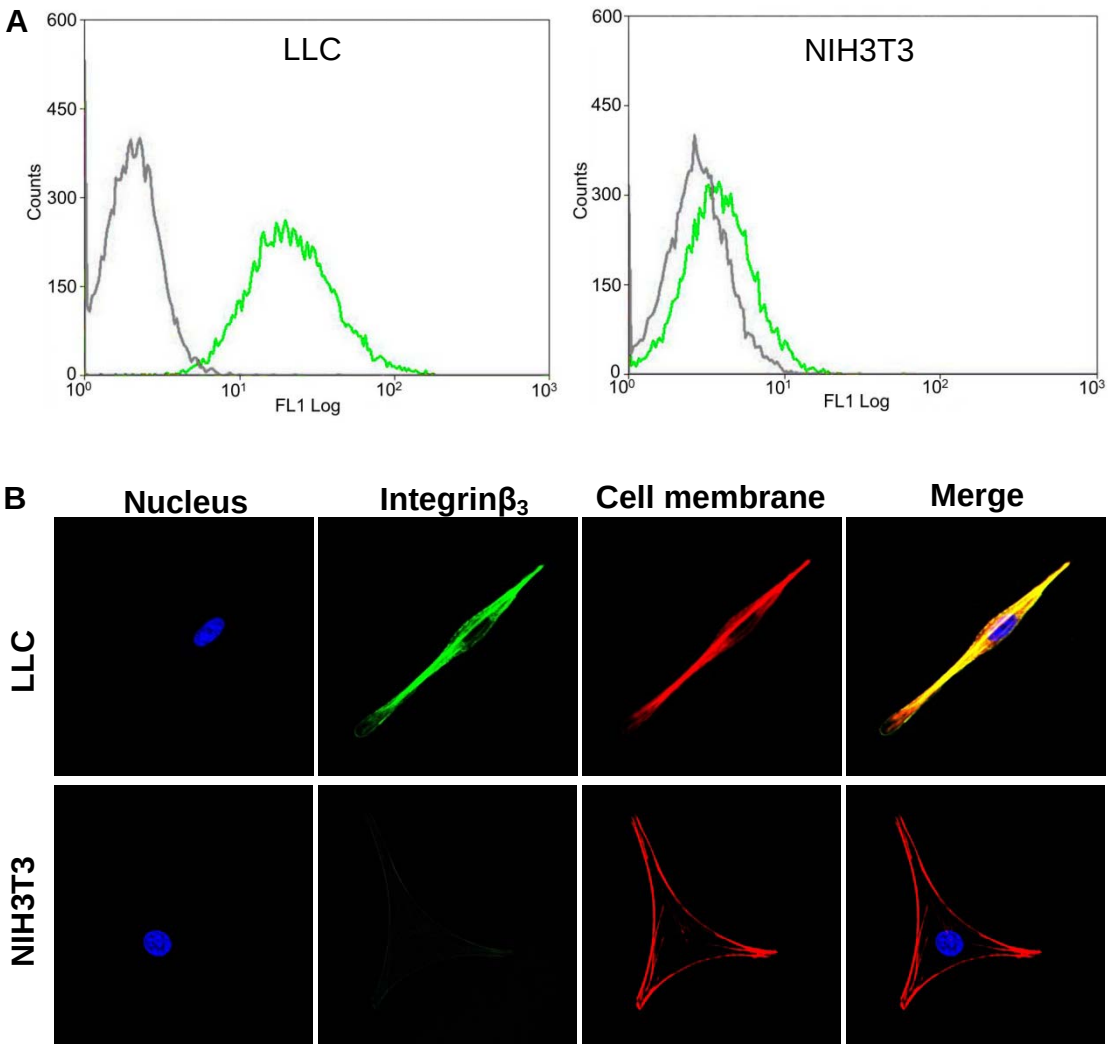


Fig. S7. FACS analysis (A) and CLSM images (B) of the expression of $\beta_3$ integrin in LLC and NIH3T3. A: Grey line: background; green line: anti-$\beta_3$.

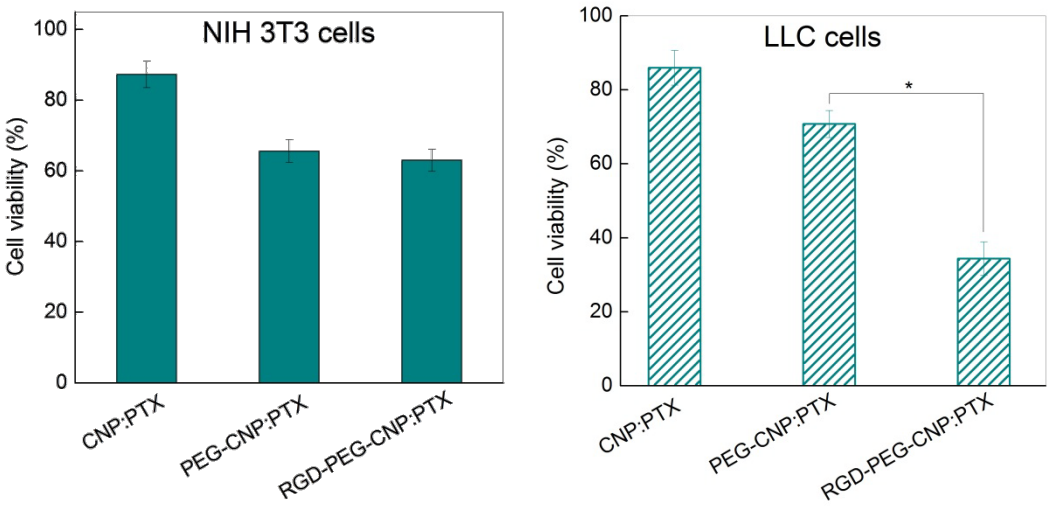


Fig. S8. The cytotoxicity of different PTX-loaded nanoparticles (CNP:PTX, PEG-CNP:PTX and RGD-PEG-CNP:PTX) against the NIH 3T3 and LLC cells when the PTX concentration was 5 μg/mL. *P<0.05.

As shown in Fig. S8, there was no significant difference in cytotoxicity between PEG-CNP:PTX and RGD-PEG-CNP:PTX group against NIH3T3 cells. However, the cytotoxicity of RGD-PEG-CNP:PTX towards LLC cells significantly increased in comparison with PEG-CNP:PTX (P<0.05). This is because RGD could bind preferentially to the integrin that is highly expressed on the surface of LLC cells (Fig. S7), increasing cellular uptake amount of RGD-PEG-CNP:PTX.

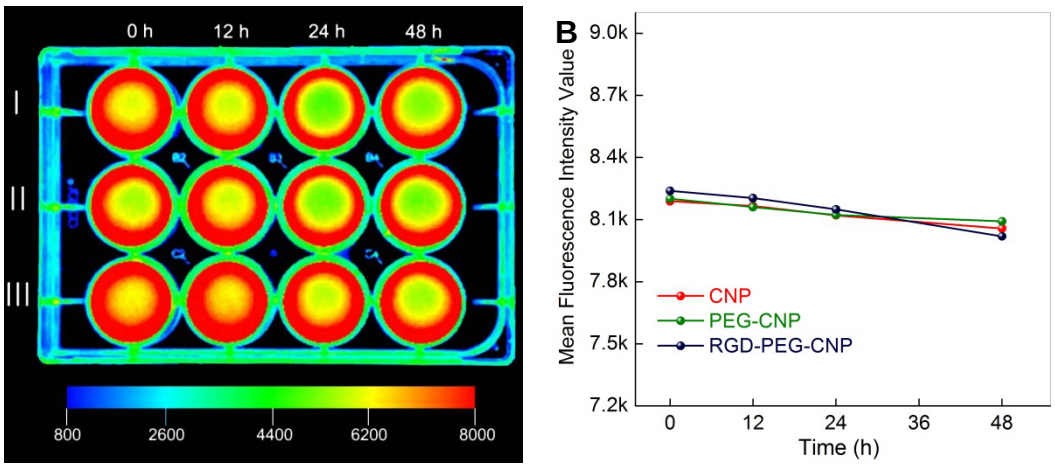


Fig. S9. The stability evaluation of DIR complexes with different nanoparticles. A: Thefluorescence images of different DIR-loaded nanoparticles (I: CNP, II: PEG-CNP, III: RGD-PEG-CNP); B: The time variation of fluorescence intensity for different DIR-loaded nanoparticles.

Method: Three complexes (CNP:DIR, PEG-CNP:PTX and RGD-PEG-CNP:PTX) were dispersed into PBS (pH7.2, 0.5 mg/mL) and incubated at 37 $^{o}$C under gentle shaking at 120 rpm. After incubation for different time intervals, these complexes were washed three times by PBS, redispersed into 1 mL PBS, transferred to a 12-well plate, and detected by In-vivo Imaging System to quantify corresponding fluorescence intensity. The wavelengths of excitation filter and emission filter were 750 nm and 790 nm, respectively.

Result: As shown in Fig. S9, the fluorescence intensity of DIR complexes with nanoparticles did not significantly decrease within 48 h, indicating their favorable stability.

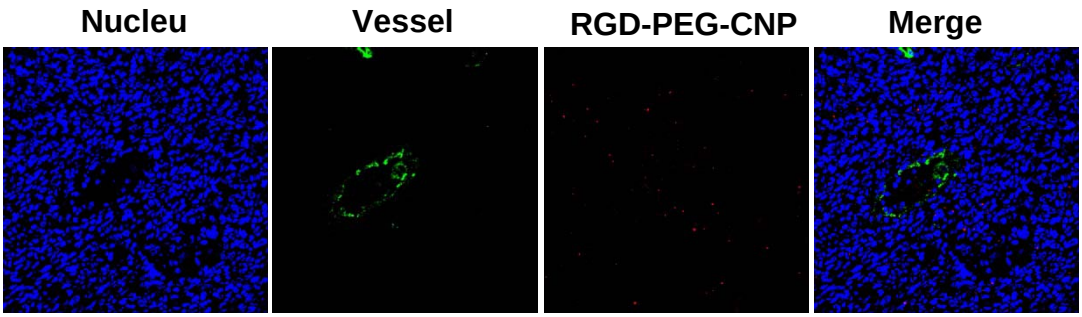


Fig. S10: The distribution of RGD-PEG-CNP in tumor tissue. The nucleus, vessel and RGD-PEG-CNP were stained with DAPI, Rat monoclonal antibody to mouse CD31 (purchased from invitrogen) and hydrophobic Cyanine 5 (Cy5), respectively.The corresponding fluorescent images at 420-450 nm, 500-560 nm, and 650-700 nm were taken by CLSM. The Cy5 was loaded into RGD-PEG-CNP by the same method of PTX loading.

References:

(1) Chen,X. G.; Park,H. J. *Carbohyd. Polym.***2003**, *53*, 355-359.

(2) A. Mandal, V. Meda, W. J. Zhang, K. M. Farhan, A. Gnanamani.*Colloids Surf. B. Biointerfaces***2012,***1*, 191-196.